

Numerical study for forecasting the dam break flooding flows impacts on different shaped obstacles

Issakhov A.A., Mussakulova G.

Abstract— This paper presents numerical study for forecasting the dam break flooding flows impacts on different shaped obstacles. A mathematical model for simulation of flooding flow is based on Navier-Stokes equations coupled with the volume-of-fluid (VOF) method. The 2D computational domain is discretized via the finite volume method (FVM). For turbulence modelling, the model is chosen. The interface between air and liquid is captured by CICSAM (compressive interface capturing scheme for arbitrary meshes) scheme, whereas the semi-implicit method for pressure linked equations (SIMPLE) scheme is applied for the pressure-velocity coupling. A second order upwind discretization scheme is used for the momentum equations. The verification of the present results is produced on a single flooding water body. The results show a good agreement with previous simulations and experiments of different authors. Then the simulation is expanded and analysed for cases with two different types of obstacles. Numerical simulation results are illustrated by figures and tables.

Keywords— Navier-Stokes equations, phase equation, mathematical model, hydraulic constructions, dam break.

I. INTRODUCTION

DAMS are the structures designed to partition a watercourse or water for the lifting of the water level, in order to concentrate a water pressure at the site of construction and to create a reservoir. Typically, dams are parts of the hydroelectric complex, i.e., hydraulic structures, which are built in a particular location for the use of water resources for specific purposes: irrigation, hydropower, irrigation of pastures and so on.

The type and design of the dam are determined by its size, purpose, and the natural conditions and the main building material. Dams differ in the type of the basic material from which they are erected, purpose and water passing conditions.

By the purpose of use, dams are divided into storage reservoir and water level pumping types. Water pumping dams are built to improve the conditions of water intake from the river, the use of water power and so on. Therefore, affluent of

the water level of this type of dams is low. The storage dams are characterised by a much higher altitude, which leads to creating a large volume of the reservoir. A distinctive feature of large storage dams is the ability to regulate the flow, small dams, by which, for example, ponds are created, does not regulate the flow.

As an alternative to the division of dams by their purposes acts division of dams by the height of water rise: low-pressure (depth of the water before the dam to 15 m), middle-pressure (15-50 m), high-pressure (over 50 m).

By the type of the material, dams are divided into ground, tabby, metal, fabric, wood, iron-tabby, gabion types. By the way of perception of the main loads: gravity, arch, buttress, arch-gravity.

Nowadays, potential catastrophic floods, resulting as an outcome of dam destructions, make great concern, since they bring huge damage. The proof of this is seen in already occurred accidents. Dam accidents bring great damage, lead to the loss of human and financial resources. In order to minimise possibilities of such accidents a mathematical modelling is used, which allows making small financial cost experiments, which results are very close to reality.

II. BACKGROUND

Mathematical modelling is also used in cases of accidents at the dams, to maximise the "softening" of the aftermath. Selection of the most appropriate model and methods for simulating floods, caused by breakout, are very important steps. Also one should take into account that one-dimensional and two-dimensional models, compared to the three-dimensional model, have limitations, such as the failure of the first to embrace the spatial extent of the flood, from the standpoint of flow depth, velocity, time of arrival and flood recession, etc. Nowadays, as a result of the development of technologies, parallel computation is also developed, which, as it is known, allows spending less time for simulations. Thus, in the papers [1, 2], a mathematical model of a dam break problem is also provided and developed an improved method for correction of the pressure, in conjunction with the volume of fluid method and the immersed boundary, to improve

This work is supported by grant from the Ministry of education and science of the Republic of Kazakhstan.

A. Issakhov al-Farabi Kazakh National University, 050040, Almaty, Kazakhstan (e-mail: alibek.issakhov@gmail.com)

G. Mussakulova al-Farabi Kazakh National University, 050040, Almaty, Kazakhstan (e-mail: milanakusakina@gmail.com)

multiphase flow calculations. TFQMR (The Transpose-Free Quasi-Minimal Residual) algorithm [2] is used to reduce the processing time in the Poisson equation solution.

In addition to the methods described in the papers mentioned above, there are also many other numerical methods for the dam break problems. So the integral boundaries method are described in papers [3-5], front track method in papers [6-8], the volume of fluid method [1, 2, 9, 10], the lattice Boltzmann method [11-13], the specified level method [14- 16], the phase-field methods [17-20].

III. MATHEMATICAL MODEL

Reynolds-Averaged Navier-Stokes equations form the basis of the present mathematical model. Application of the Boussinesq approximation leads to the following system of equations, where for turbulence modelling the $k - \varepsilon$ model is chosen [21]:

$$\frac{\partial u_j}{\partial x_j} = 0$$

$$\rho \frac{\partial u_i}{\partial t} + \rho u_j \frac{\partial u_i}{\partial x_j} = -\frac{\partial P}{\partial x_j} + \frac{\partial}{\partial x_j} \left[(\mu + \mu_t) \frac{\partial u_i}{\partial x_j} \right] + \rho \bar{g}$$

$$\frac{\partial \phi}{\partial t} + \frac{\partial \phi u_i}{\partial x_j} = 0$$

$$\rho = \phi \rho_1 + (1 - \phi) \rho_2$$

$$\mu = \phi \mu_1 + (1 - \phi) \mu_2$$

$$\mu_T = \rho C_\mu \frac{k^2}{\varepsilon}$$

$$\rho \frac{\partial k}{\partial t} + \rho u_j \frac{\partial k}{\partial x_j} = -\tau_{ij} \frac{\partial u_i}{\partial x_j} - \rho \varepsilon + \frac{\partial}{\partial x_j} \left[\left(\mu + \frac{\mu_t}{\sigma_k} \right) \frac{\partial k}{\partial x_j} \right] +$$

$$\frac{\mu_t}{\rho P_{rt}} \left(-g_x \frac{\partial P}{\partial x} - g_y \frac{\partial P}{\partial y} \right)$$

$$\rho \frac{\partial \varepsilon}{\partial t} + \rho u_j \frac{\partial \varepsilon}{\partial x_j} = C_{\varepsilon 1} \frac{\varepsilon}{k} \tau_{ij} \frac{\partial u_i}{\partial x_j} - C_{\varepsilon 2} \rho \frac{\varepsilon^2}{k} +$$

$$C_{\varepsilon 1} \frac{\varepsilon}{k} C_{\varepsilon 3} \frac{\mu_t}{\rho P_{rt}} \left(-g_x \frac{\partial P}{\partial x} - g_y \frac{\partial P}{\partial y} \right) + \frac{\partial}{\partial x_j} \left[\left(\mu + \frac{\mu_t}{\sigma_\varepsilon} \right) \frac{\partial \varepsilon}{\partial x_j} \right]$$

where u_j are the velocity components, x_j are the Cartesian coordinate directions, P is the pressure, ϕ is the volume fraction, ρ is the mixture density, ρ_1 and ρ_2 are the densities of air and water, respectively, μ_t is the turbulent viscosity, μ is the viscosity, μ_1 and μ_2 are the viscosities of air and water, respectively, k is the turbulent kinetic energy, ε is the dissipation rate, τ_{ij} is the Reynolds stress tensor, C_μ , σ_k , $C_{\varepsilon 1}$, $C_{\varepsilon 2}$, σ_ε are closure coefficients: $C_{\varepsilon 1} = 1.44$, $C_{\varepsilon 2} = 1.92$, $C_\mu = 0.09$, $\sigma_k = 1.0$, $\sigma_\varepsilon = 1.3$.

IV. NUMERICAL ALGORITHM

For the numerical simulation of the system of equation discussed on section 3 the SIMPLE (Semi-Implicit Method for Pressure Linked Equations) algorithm is applied. This algorithm was first developed by B. Spalding and S. Patankar [25-36].

V. A SINGLE FLOODING WATER BODY IN A SQUARE RESERVOIR

In this section, a dam break experiment described in papers [22-24] is repeated in order to validate present simulations. The geometry of the experiment given in figure 1 is performed as a tank with measuring 3.22×2 m.

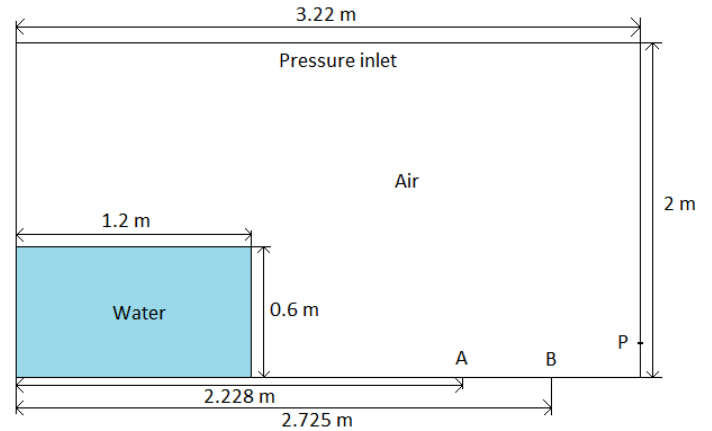


Figure 1 – The geometry of simulation model.

58464 quadrilateral structured grids with the maximum face size 0.002 m are used in the computational domain. A steady time step $dt = 0.001$ s is chosen.

Validation is done via the comparison of present water height history results at points A and B located at $x = 2.228$ m, $x = 2.725$ m, with those from the paper [22].

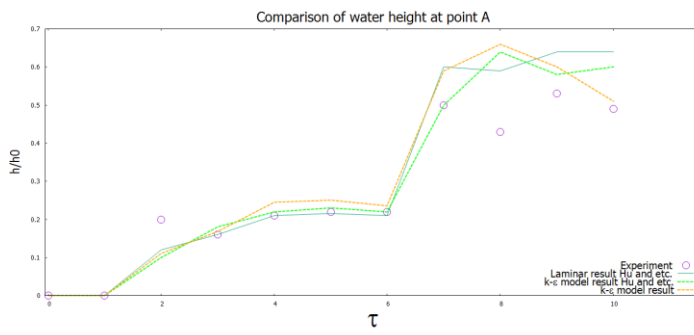


Figure 2 - Comparison of the water height h_1 at point A with numerical simulation results and experimental data [22].

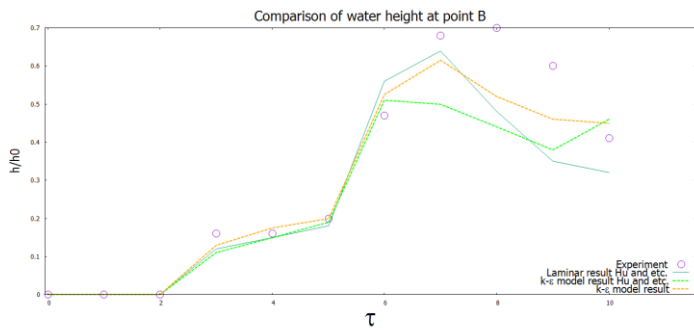


Figure 3 - Comparison of the water height h_2 at point B with numerical simulation results and experimental data [22].

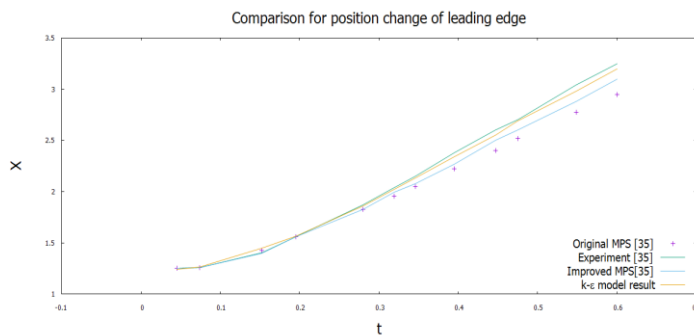


Figure 4 - Comparison of the water front with numerical simulation results and experimental data [23].

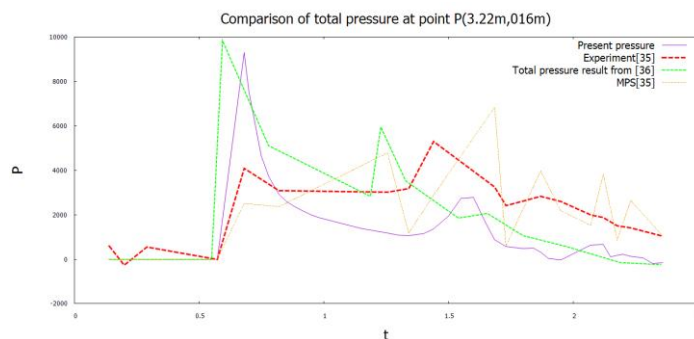


Figure 5 – Comparison of pressure impact against downstream wall at point $P(3.22m,0.16m)$ with numerical simulation results and experimental data.

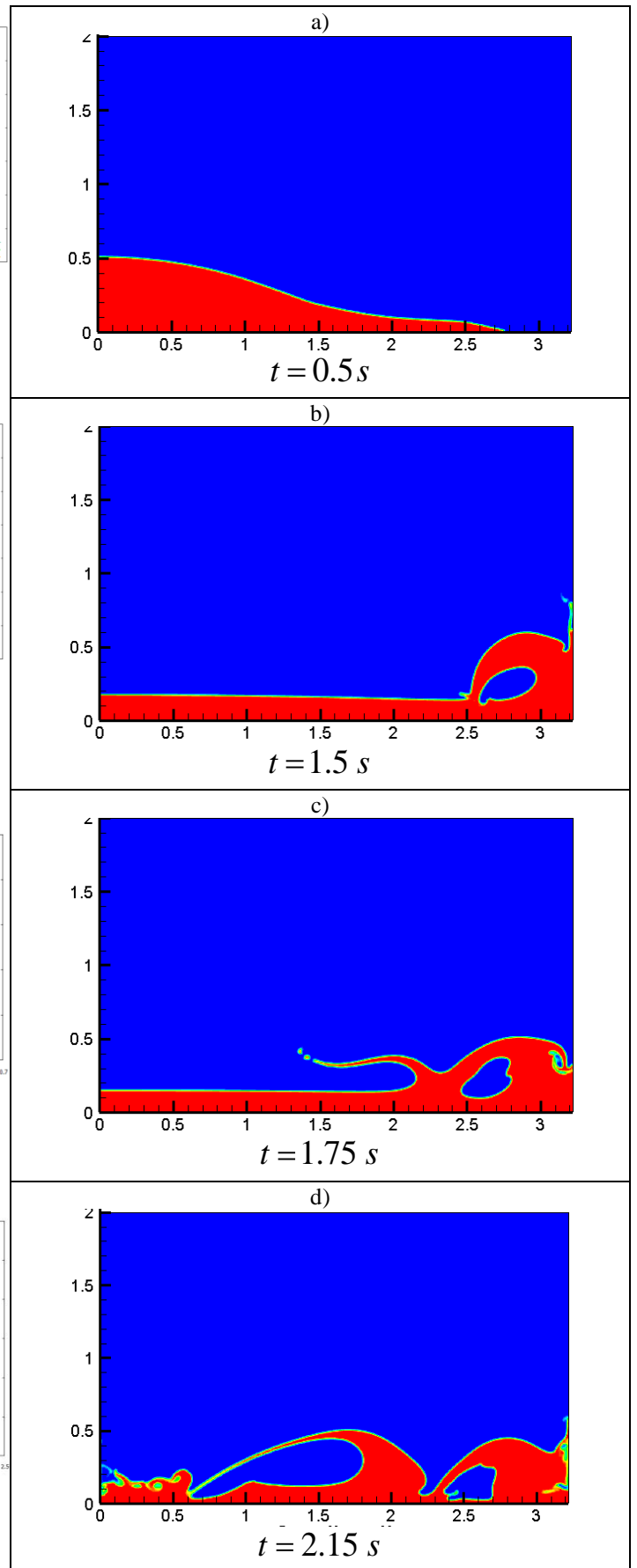


Figure 6 - Free surface evolution.

The time t is nondimensionalized as $\tau = t\sqrt{2g/h_0}$ and $h_0 = 0.6m$. The comparison of the interface snapshots in Figures 2 and 3 demonstrate good verification of the present $k-\varepsilon$ model.

In Figures 2 and 3 the computed water heights h_1, h_2 at the points A and B at ten times stepping process compared to the results from the paper [22]. The present simulation results are in good agreement with numerical simulation results and experimental data [22].

The time history of water front toe evolution is also compared with the results from another research paper [23] as shown in figure 4 and show good agreement with numerical simulation results and experimental data. Figure 5 shows the time history of the pressure at the point $P(3.22m, 0.16m)$ [23, 24]. Four lines of graphs are seen in the figure show the experimental and MPS results provided from [23], total pressure results from [24]. Since there only a few time history values of pressure at this point are taken, for the sake of simplicity, given line graphs might seem not smooth enough, but all important values of point P, i.e. its peaks, provided in papers [23, 24] and presented simulation are taken into account.

Overall, all results predict the two pressure peaks at about the same time instants. The snapshots of a single flooding water body in a square tank simulation at 6 different time instants are shown in figure 6.

VI. IMPACT OF FLOODING FLOW ON A RECTANGULAR OBSTACLE

In this section impact of flooding flow on a rectangular obstacle is studied. The dimensions of the computational domain, liquid body and the flap are shown in figure 7. The size of the reservoir this time is $0.584 \times 0.584 m^2$. A water body with an initial height $h_0 = 0.292 m$ and width $l_0 = 0.146 m$ is located on the left side of the reservoir. 170518 quadrilateral structured grids with the maximum face size $0.002 m$, $dt = 0.001 s$ are used for numerical computations.

In order to avoid repetitions in descriptions of each numerical experiment, let's discuss common conditions for all of them.

As the primary phase the air at standard atmospheric condition is chosen, whilst fresh water at $T = 20^\circ C$ is chosen as the secondary phase. The nonslip wall condition, which implies the fluid to stick to the wall, is set on all the boundaries except the top one on which an opening boundary is imposed. For the volume fraction equation, Neumann's boundary condition is set.

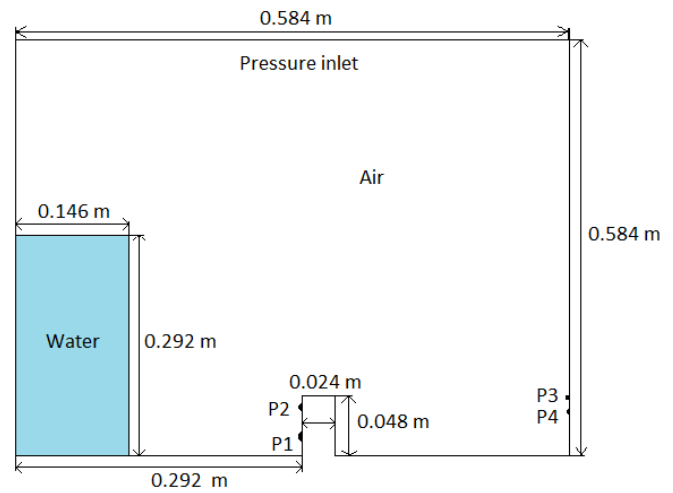


Figure 7 – The geometry of simulation model.

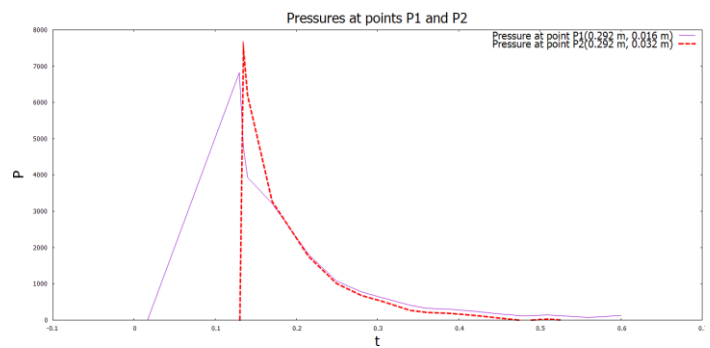


Figure 8 – Impact of pressures at points P_1 and P_2 .

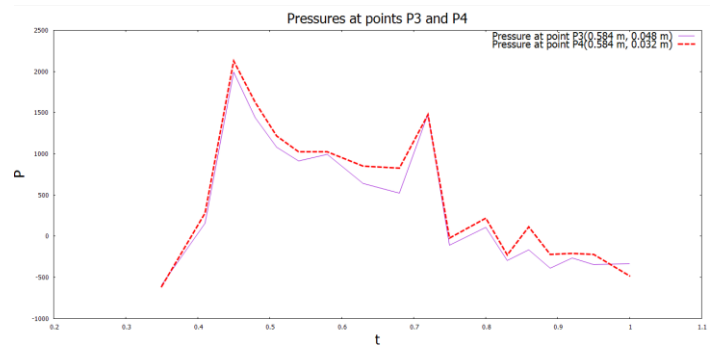


Figure 9 – Impact of pressures at points P_3 and P_4 .

Figure 8 shows the variation of pressure at points $P_1(0.292m, 0.016m)$ and $P_2(0.292m, 0.032m)$. The pressure peaks happen when the collapsed water column arrives at the obstacle at about $0.13 s$, then the pressure decreases to the hydrostatic pressure.

While in figure 9, the pressure jumps due to the strong discontinuity of water jet, that is why the peaks at points $P_3(0.584m, 0.048m)$ and $P_4(0.584m, 0.032m)$ repeat many times, but their values are smaller compare to P_1 and P_2 .

The investigation of pressure peaks is crucial for the choice of dam material and its sizes since at large pressure peaks a

dam of a certain thickness and material may not withstand and can failure.

The three snapshots of numerical simulation of a single flooding water body in a square tank with an obstacle at different time instants are illustrated in figure 10.

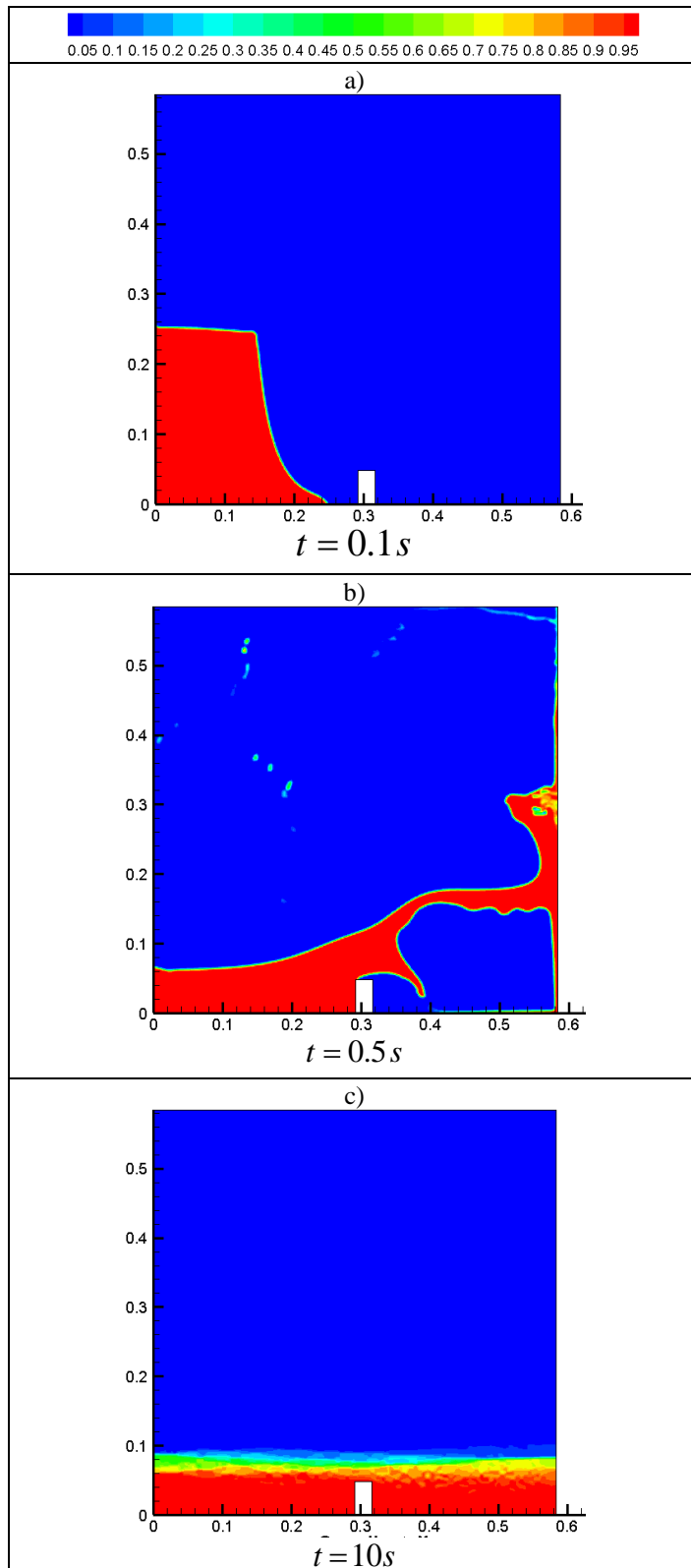


Figure 10 – Impact of a water flow on a rectangular obstacle.

VII. IMPACT OF FLOODING FLOW ON A TRAPEZOIDAL OBSTACLE

In the present section impact of flooding flow on a trapezoidal obstacle is considered. The dimensions of the computational domain, liquid body and the flap are shown in figure 11. The size of the reservoir this time is $0.584 \times 0.584 \text{ m}^2$. A water body with an initial height $h_0 = 0.292 \text{ m}$ and width $l_0 = 0.146 \text{ m}$ is located on the left side of the reservoir. 170328 quadrilateral structured grids with the maximum face size 0.002 m , $dt = 0.001 \text{ s}$ are used for numerical computations.

As can be seen from the comparison of tables 1 for rectangular and trapezoidal obstacles, the shape of a dam play one of the key roles, since pressure peaks provided in table 1 are of higher magnitude, which is explained by the increase of an area affected by impacting water flow.

In this experiment pressure peak along the left wall of the obstacle occurs at $t = 0.135 \text{ s}$. As time goes on a small liquid tongue forms above the obstacle and at the time approximately $t = 0.35 \text{ s}$, the jet impinges the right wall of the tank, entrapping the area beneath it. After some fluctuations the system comes to an equilibrium state.

Figure 12 shows three snapshots of a numerical simulation of an impact of water flow on a trapezoidal obstacle. Figure 13 illustrates the impact of pressure by water flow on rectangular and trapezoidal obstacles.

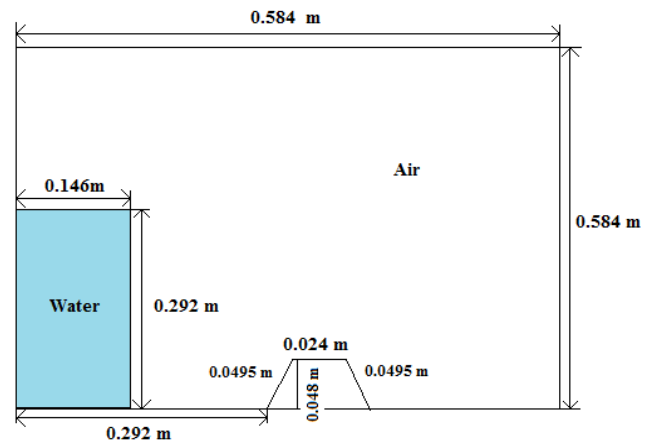


Figure 11 – The geometry of the simulation model.

t (time, s)	trapezoidal obstacle		rectangular obstacle	
	P (pressure, Pa)	Y (y- coordinate, m)	P (pressure, Pa)	Y (y- coordinate, m)
0.13	5240	0.015	6740	0.0159
0.135	5766	0.0267	7398	0.03
0.14	5585	0.0364	7141	0.04
0.145	5312	0.0456	6715	0.0459
0.15	4837	0.0459	5611	0.046
0.155	4340	0.0459		

Table 1 – Pressure peaks along the left wall of the different shape obstacles.

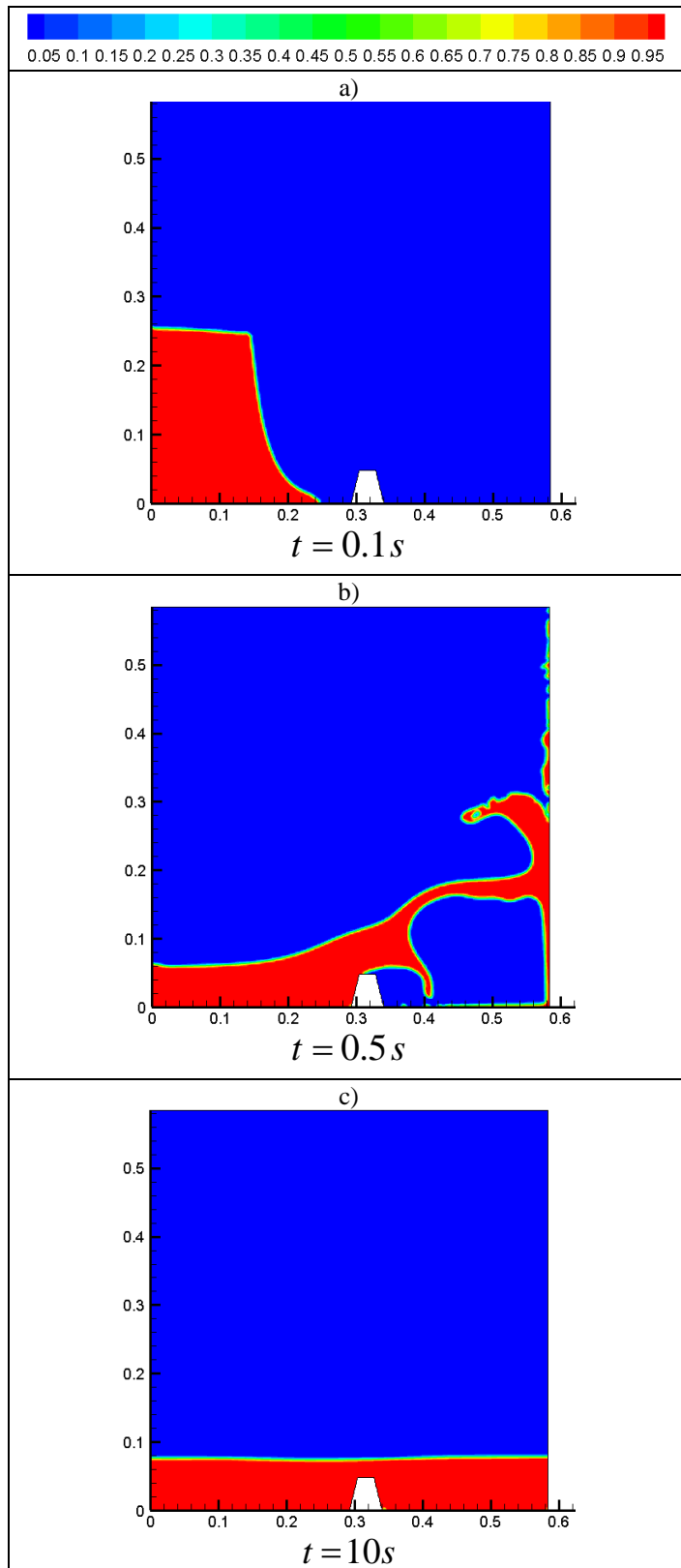


Figure 12 - Impact of a water flow on a trapezoidal obstacle.

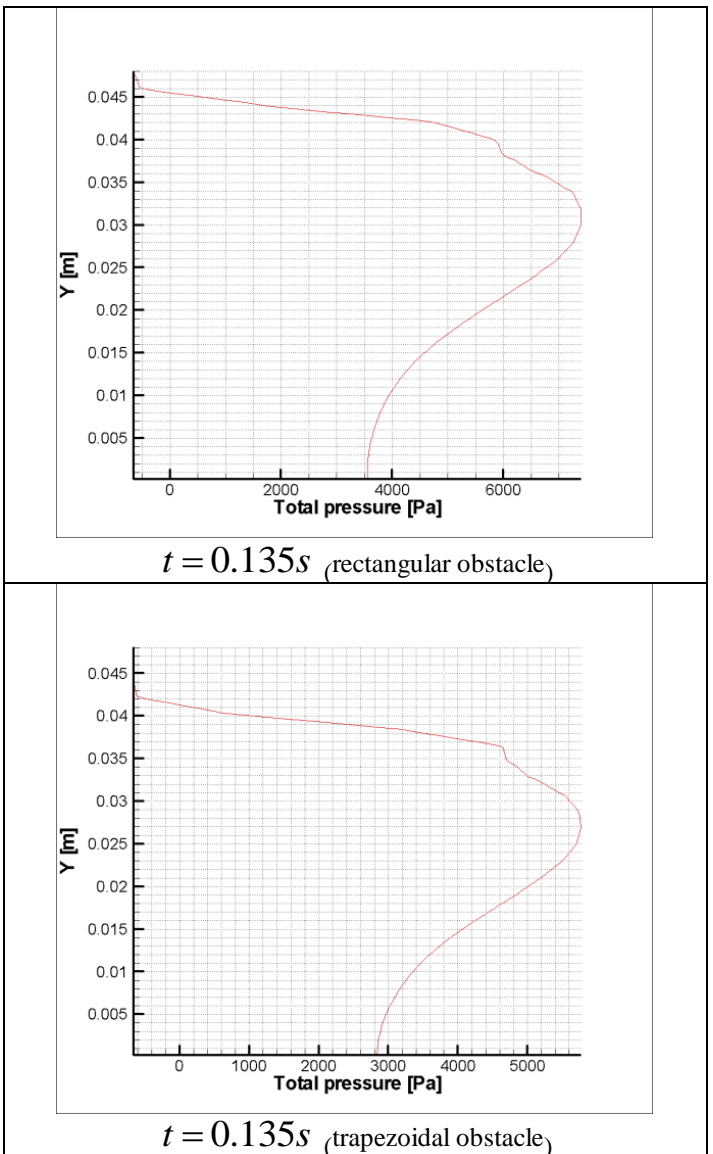


Figure 13 - Impact of a water flow on a rectangular and trapezoidal obstacle, pressure fronts.

VIII. CONCLUSION

In the present paper, the interface evolution of flooding flow and impacts of liquid on two different shape of obstacles were simulated using a Navier-Stokes solver with a VOF-based interface capture scheme. The application of the $k - \epsilon$ turbulence model was also considered. Although comparisons of experiment results with numerical simulation results and experimental data from [22-24] show some differences, present simulation can give reasonable results of the dam breaking problem and can capture the principal features of the interface evolution. So, the present numerical simulation technique can be applied for prediction of the hydrodynamics of structures with water flow impact.

Based on the numerical results obtained, it can be concluded that the building of a dam plays an important role not only in building materials but also in the form of the dam itself. Since, using a certain dam form, it will be possible to

reduce the pressure created by a large volume of water on the wall of the dam. When selecting certain forms of dam walls, it will be possible to use not so durable building materials, which is economically costly. In this paper, by using the numerical simulation, the efficiency of using a dam with trapezoidal walls is shown. When this form is used, the pressure on the walls of the dam is 1.28 less than in the case of a rectangular wall, which is more cost effective. In the future, when constructing new dams, it will be possible to save, for example, on the thickness of dam walls, building materials, etc., but at the same time have the same endurance of dam walls as with a rectangular shape.

VI. ACKNOWLEDGMENT

This work is supported by the grant from the Ministry of education and science of the Republic of Kazakhstan.

REFERENCES

- [1]. Biscarini C., Di Francesco S., Manciola P. "CFD modeling approach for dam break flow studies". *Hydrology and Earth System Sciences* 2010; 14:705-718.
- [2]. Lin S.-Y., Yang F.-L., Chen C.-S., Hsieh S.-H. "A parallel VOF IB pressure-correction method for simulation of multiphase flows". *Applied Mathematical Modelling* 2016; 40:1800-1815.
- [3]. Baker G.R., Meiron D.I., Orszag S.A. "Vortex simulations of the Rayleigh-Taylor instability". *Physics of Fluids* 1980; 23:1485-1490.
- [4]. Duchemin L., Josserand C., Calvin P. "Asymptotic behavior of the Rayleigh-Taylor instability". *Physical Review Letters* 2005; 94:224501-1-224501-4.
- [5]. Verdon C.P., McCrory R.L., Morse R.L., Baker G.R., Meiron D.I., Orszag S.A. "Nonlinear effects of multifrequency hydrodynamic instabilities on ablatively accelerated thin shells". *Physics of Fluids* 1982; 25:1653-1674.
- [6]. Popinet S., Zaleski S. "A front-tracking algorithm for accurate representation of surface tension". *International Journal for Numerical Methods in Fluids* 1999; 30:775-793.
- [7]. Tryggvason G., Bunner B., Esmaeeli A., Juric D., Al-Rawahi N., Tauber W., Han J., Nas S., Jan Y.-J. "A front-tracking method for the computations of multiphase flow". *Journal of Computational Physics* 2001; 169:708-759.
- [8]. Univerdi S.O., Tryggvason G. "A front-tracking method for viscous, incompressible, multi-fluid flows". *Journal of Computational Physics* 1992; 100:25-37.
- [9]. Gerlach D., Tomar G., Biswas G., Durst F. "Comparison of volume-of-fluid methods for surface-tension dominant two-phase flows". *International Journal of Heat and Mass Transfer* 2006; 49:740-754.
- [10]. Hirt C.W., Nichols B.D. "Volume of fluid (VOF) method for the dynamics of free boundaries". *Journal of Computational Physics* 1981; 39:201-225.
- [11]. He X., Chen S., Zhang R. "A lattice Boltzmann scheme for incompressible multiphase flow and its application in simulation of Rayleigh-Taylor instability". *Journal of Computational Physics* 1999; 152:642-663.
- [12]. He X., Zhang R., Chen S., Doolen G.D. "On the three-dimensional Rayleigh-Taylor instability". *Physics of Fluids* 1999; 11:1143-1152.
- [13]. Nie X., Qian Y.-H., Doolen G.D., Chen S. "Lattice Boltzmann simulation of the two-dimensional Rayleigh-Taylor instability". *Physical Review E* 1998; 58:6861-6864.
- [14]. Chang Y.C., Hou T.Y., Merriman B., Osher S. "Eulerian capturing methods based on a level set formulation for incompressible fluid interfaces". *Journal of Computational Physics* 1996; 124:449-464.
- [15]. Gomez P., Hernandez J., Lopez J. "On the reinitialization procedure in a narrow-band locally refined level set method for interfacial flows". *International Journal for Numerical Methods in Engineering* 2005; 63:1478-1512.
- [16]. Sussman M., Smereka P., Osher S. "A level set approach for computing solutions to incompressible two-phase flow". *Journal of Computational Physics* 1994; 114:146-159.
- [17]. Celani A., Mazzino A., Muratore-Ginanneschi P., Vozella L. "Phase-field model for the Rayleigh-Taylor instability of immiscible fluids". *Journal of Fluid Mechanics* 2009; 622:115-134.
- [18]. Ding H., Spelt P.D.M., Shu C. "Diffuse interface model for incompressible two-phase flows with large density ratios". *Journal of Computational Physics* 2007; 226:2078-2095.
- [19]. Jacqmin D. "Calculation of two-phase Navier-Stokes flows using phase-field modeling". *Journal of Computational Physics* 1999; 155:96-127.
- [20]. Anderson J.D. *Computational Fluid Dynamics. The Basics with Applications*. 1995. p. 547
- [21]. Chung T.J. *Computational fluid dynamics*. // CUP, 2002.
- [22]. Hu J., Lu Z.Q., Kan X.Y., Sun S.L. "Numerical Simulation on Interface Evolution and Impact of Flooding Flow". *Shock and Vibration* 2015.
- [23]. Qiao-rui W., Tan M., Xing J. An improved moving particle semi-implicit method for dam break simulations. *Journal of Ship Mechanics* 2014.
- [24]. Abdolmaleki K., Thiagarajan K., Morris-Thomas M. "Simulation of the dam break problem and impact flows using a Navier-Stokes solver". 15th Australasian fluid Mechanics Conference 13-17 December 2004.
- [25]. Patankar, S. V., Spalding, D.B. "A calculation procedure for heat, mass and momentum transfer in three-dimensional parabolic flows", *Int. J. of Heat and Mass Transfer*, Volume 15, Issue 10, 1972, pp. 1787-1806.

- [26]. Issakhov A. "Mathematical Modelling of Thermal Process to Aquatic Environment with Different Hydrometeorological Conditions". *The Scientific World Journal*, vol. 2014, Article ID 678095, 10 pages, 2014. doi:10.1155/2014/678095
- [27]. Issakhov A. "Modeling of Synthetic Turbulence Generation in Boundary Layer by Using Zonal RANS/LES Method". *International Journal of Nonlinear Sciences and Numerical Simulation*. Volume 15, Issue 2, Pages 115–120, DOI: 10.1515/ijnsns-2012-0029, 2014
- [28]. Issakhov A. "Mathematical Modeling of the Discharged Heat Water Effect on the Aquatic Environment from Thermal Power Plant". *International Journal of Nonlinear Sciences and Numerical Simulation*. Volume 16, Issue 5, Pages 229–238, DOI: 10.1515/ijnsns-2015-0047, June 2015
- [29]. Issakhov A. "Mathematical modeling of the discharged heat water effect on the aquatic environment from thermal power plant under various operational capacities". *Applied Mathematical Modelling*, Volume 40, Issue 2, 15 January 2016, Pages 1082–1096
- [30]. Issakhov A. "Mathematical Modelling of the Thermal Process in the Aquatic Environment with Considering the Hydrometeorological Condition at the Reservoir-Cooler by Using Parallel Technologies". *Sustaining Power Resources through Energy Optimization and Engineering*, Editors: Vasant, Pandian, and Nikolai Voropai. IGI Global, 2016, pp. 1-494, doi:10.4018/978-1-4666-9755-3, Chapter 10, 2016, pp. 227-243, DOI: 10.4018/978-1-4666-9755-3.ch010
- [31]. Issakhov A. "Numerical modelling of distribution the discharged heat water from thermal power plant on the aquatic environment". *AIP Conference Proceedings* 1738, 480025 (2016); doi: 10.1063/1.4952261.
- [32]. Issakhov, A.; "Mathematical Modelling of the Influence of Thermal Power Plant on the Aquatic Environment with Different Meteorological Condition by Using Parallel Technologies". *Power, Control and Optimization. Lecture Notes in Electrical Engineering*. 239, 165–179 (2013).
- [33]. Issakhov A. "Numerical modelling of the thermal effects on the aquatic environment from the thermal power plant by using two water discharge pipes". *AIP Conference Proceedings* 1863, 560050 (2017); doi: <http://dx.doi.org/10.1063/1.4992733>
- [34]. Issakhov, A.; "Mathematical modelling of the influence of thermal power plant to the aquatic environment by using parallel technologies". *AIP Conf. Proc.* 1499, 15–18, (2012), doi: <http://dx.doi.org/10.1063/1.4768963>
- [35]. Issakhov, A.; "Numerical study of the discharged heat water effect on the aquatic environment from thermal power plant by using two water discharged pipes," *International Journal of Nonlinear Sciences and Numerical Simulation*. 18(6): 469-483, (2017). <https://doi.org/10.1515/ijnsns-2016-0011>.
- [36]. Issakhov, A.; "Numerical modeling of the effect of discharged hot water on the aquatic environment from a thermal power plant". *International Journal of Energy for a Clean Environment*, Volume 16, Issue 1-4, 2015, pages 23-28, DOI: 10.1615/InterJEnerCleanEnv.2016015438